iJRASET
International Journal For Research in Applied Science and Engineering Technology

INTERNATIONAL JOURNAL FOR RESEARCH

IN APPLIED SCIENCE & ENGINEERING TECHNOLOGY

Volume: 9 **Issue:** I **Month of publication:** January 2021

DOI: https://doi.org/10.22214/ijraset.2021.32720

www.ijraset.com

Call: 08813907089 | E-mail ID: ijraset@gmail.com

International Journal for Research in Applied Science & Engineering Technology (IJRASET)
ISSN: 2321-9653; IC Value: 45.98; SJ Impact Factor: 7.429
Volume 9 Issue I Jan 2021- Available at www.ijraset.com

Numerical Analysis of De Laval Nozzle under Surrounding Zone and Compressed Flow

Mohd Shais Khan[1], Syed Asim Minhaj[2]
[1, 2]*BE, Dept of Mechanical Engineering, Muffakham Jah College of Engineering and Technology*

Abstract: ***The research paper simulates airflow in a supersonic De Laval nozzle and explores air flow actions isolated from the local area's nozzle. The pressure levels in the input portion of the nozzle (pressure-inlet condition) and the atmospheric output parts (pressure-outlet condition) are used to replicate the current model. The fluid divides the motion of a lambda shock, led to a series of expansion and compression waves; for 1:4 < NPR < 2:4, the estimation shows the probability of an asymmetric flow structure. Computationally obtained asymmetric flow models are compatible with previous theoretical flow visualization studies. The nozzle pressure ratio (NPR) is equivalent to balancing the nozzle's inlet air pressure to the ambient pressure. Thus, the value of the nozzle pressure ratio in the current system is 1.5, and the amount of inlet air pressure and the pressure at the output is equal to the ambient pressure. The data contrast review indicates adequate coordination between the experimental data and the simulation outcomes. The surrounding zone is also affected during the shock wave formation.***
Keywords: Computational fluid dynamics, De Laval nozzle, Supersonic, Mach number, numerical validation.

I. INTRODUCTION

The De Laval nozzle is also called convergent-divergent nozzle. CD nozzle or con-di nozzle is a tube that is nicked in the middle, carefully designing a balanced, asymmetrical oval shape. It is used to accelerate the flow of heavy, pressurised gas through it to a higher supersonic speed in the axial (thrust) direction by translating the heat energy of the flow into kinetic energy. As a result, the nozzle is commonly used in certain types of steam turbines and rocket engine nozzles. It also finds application in supersonic jet engines. The mechanical form of the nozzle makes sure that when the fluid approaches it and flows through the converging portion of the nozzle, as per the continuity equation, it allows the velocity of the moving fluid to rise by lowering the cross-section of the flow; and thus, because of the Bernoulli theorem, the fluid pressure decreases with increasing velocity. Variables such as Mach number, velocity, and pressure dependent on the motion of the fluid flow in the longitudinal direction of the nozzle. The following figure 1 demonstrates the Design of the internal layout of the CD nozzle.

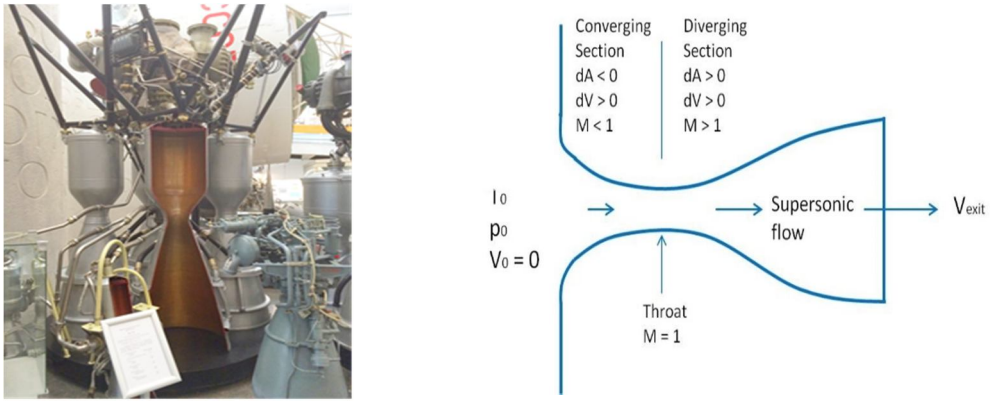

Fig. 1 Section view and details of CD nozzle

Preliminary computational analyses of separating nozzle flows, including studies performed by Hunter [1], Carlson [2], and Xiao et al. [3], demonstrate this. There is incredible satisfaction with the experimental data presented. In Hunter's analysis, which is a mixed computational and experimental investigation, two different separation regimens were found in a planar nozzle with an area-to-area exit ratio of Ae=A at 1.8. In the case of NPR < 1:8, the flow reveals a three-dimensional separation with partial reattachment. Completely detached two-dimensional axial separation is observed for NPR > 2:0. The under-expansion of the flow after the primary shock, postulated by Romine [4].

The research paper focuses more on the composition of the flow than on methods of prediction. The broad uncertainty associated with supersonic flow separation, which can be used as an excitation tool for mixing enhancement [5], motivates it in part. In this context, Papamoschou and Zill [6], who experimentally investigated the supersonic nozzle flow separation within such planar convergent-divergent nozzles that generate flows for such purposes, aim to replicate and build on the experimental findings. Their analysis reveals that the flow pattern is asymmetrical for area ratio A = 1:4 and nozzle pressure ratio NPR > 1:4, distinguished by a lambda shock with one foot often more significant than the other. During a given test run, this asymmetry does not flip but can change sides from one run to the next. From schlieren photos, the Mach stem's flow downstream was observed to Extending to near-sonic level and displaying subsonic and supersonic regions contrasting. The observational measures of the distribution of centerline pressure are qualitatively coherent with this result. It was also observed that the shock is unstable for oversized Ae = At and NPR but will not release Acoustic sounds and echo. Deck et al. [14] investigated the same planar nozzle's computational simulation With the Spalart-Allmaras turbulence model, using steady Reynolds-averaged Navier-Stokes (RANS) equations. Two asymmetric and one symmetric shock systems are calculated based on the distinct initial area used.

current study aims to research the flow structure and wave structures in the vicinity of the separation shock in computational detail to explain the salient physics and ultimately model the flow instability downstream of the shock. The Papamoschou and Zill experiment [6] is used as a framework for contrast in which symmetric or separate asymmetric flow normally exists, depending on the nozzle pressure ratio, unlike the analysis seen in Bourgoing and Reijasse[7], Bourgoing and Reijasse[8], and Deck et al.[9].

II. GEOMETRY

Using Design Modeler software, the current 2-D model is drawn. A convergent-divergent nozzle and the throat field, as well as a rectangular space containing the nozzle output, form the geometric framework of the model. It should be remembered that the ratio of the nozzle's cross-sectional area to the cross-sectional area of the throat area is estimated to be 1.5 in the present model. A view of the geometry is seen in the figure below. The meshing of the present model was performed using ANSYS Meshing tools. The form of mesh is structured, and 8000 is the element number. The grids in the region adjacent to the output of the nozzle are smaller in dimension. The mesh is seen in the following figure 2.

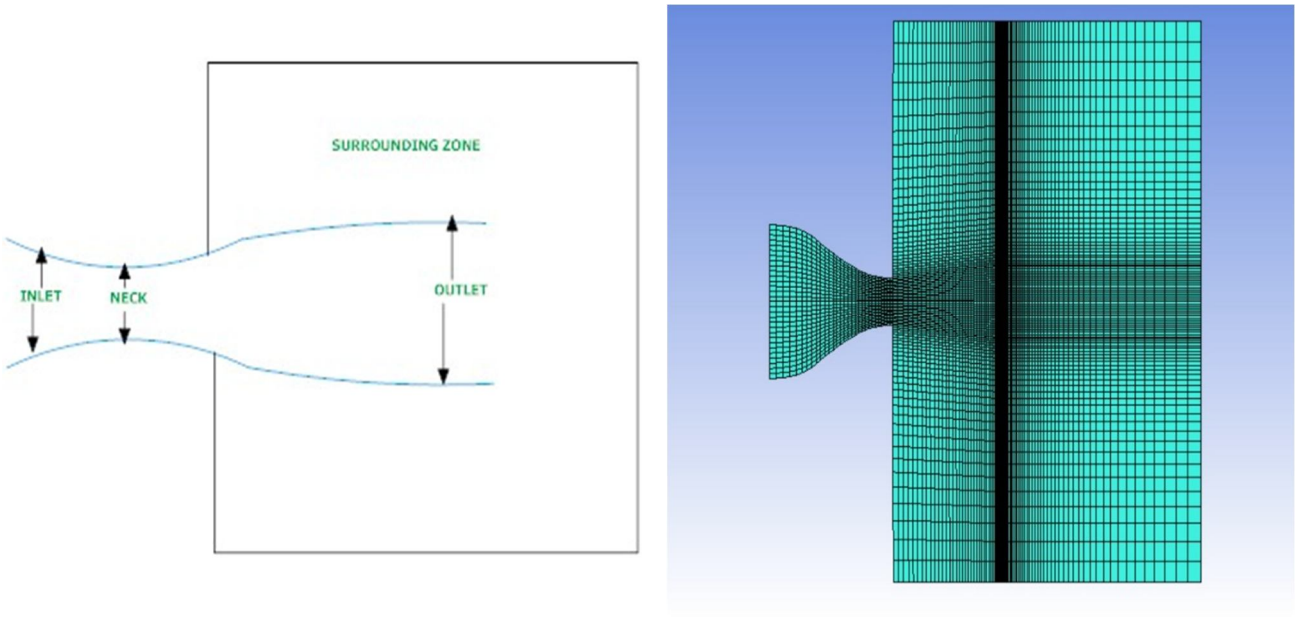

Fig. 1 Geometry and mesh used

The computing area is decomposed by subdivisions of the organised grids. Each block is treated as a single body, and only amounts of flow and instability need to be shared at the block boundaries. After in-space discretization, the. A number of ordinary differential equations with only derivatives in time are reduced to governing equations, which can be easily solved using an explicit multi-stage Runge-Kutta form of scheme. To speed up the convergence of the solution, a multigrid technique is implemented, and a second time-stepping technique is used for time-accurate erratic time marching.

III.BASIC EQUATIONS

A. The primary governing equations are the equation of conservation of mass or continuity equation and the conservation of momentum. The continuity equation or mass conservation equation in differential form is:

$$\frac{\partial \rho}{\partial t} + \nabla \cdot (\rho \mathbf{v}) = S_m \quad (1)$$

$$\frac{\partial}{\partial t}(\rho v) + \nabla \cdot (\rho v v) = -\nabla p + \nabla \cdot (\tau) + \rho g + F \quad (2)$$

B. K- Ɛ Turbulence Model The standard k-Ɛ turbulence model in ANSYS Fluent has become the workhorse of practical engineering flow calculations [13, 14]. For kinetic energy(k) turbulence and its dissipation rate (ε), the standard k- ω model is based on model transport equations. It is assumed by this model that the flow is turbulent, and other effects like molecular viscosity are negligible. Therefore, it is only valid for turbulent flows.

$$\frac{\partial}{\partial t}(\rho k) + \frac{\partial}{\partial x_i}(\rho k u_i) = \frac{\partial}{\partial x_j}\left[\left(\mu + \frac{\mu_t}{\sigma_k}\right)\frac{\partial k}{\partial x_j}\right] + G_k + G_b - \rho\varepsilon - Y_M + S_k \quad (3)$$

$$\frac{\partial}{\partial t}(\rho \varepsilon) + \frac{\partial}{\partial x_i}(\rho \varepsilon u_i) = \frac{\partial}{\partial x_j}\left[\left(\mu + \frac{\mu_t}{\sigma}\right)\frac{\partial \varepsilon}{\partial x_j}\right] + C_{1\varepsilon}\frac{\varepsilon}{k}(G_k + C_{3\varepsilon}G_b) - C_{2\varepsilon}\rho\frac{\varepsilon^2}{k} + S_\varepsilon \quad (4)$$

coefficient of laminar viscosity $\mu_t = \rho C_\mu \frac{k^2}{\varepsilon}$ (5)

In the present model, due to compressible flow and creating a pressure gradient, we use the standard k-ω turbulent model with shear flow correction capability. Model is expressed as follows:

$$\frac{\partial}{\partial t}\int_\Omega \boldsymbol{W} d\Omega + \oint_{\partial\Omega}(\boldsymbol{F}_c - \boldsymbol{F}_d) dS = \int_\Omega S d\Omega \quad (6)$$

The coefficient of laminar viscosity L by Sutherland's formula:

$$\frac{\mu_L}{\mu_{\text{ref}}} = \left(\frac{T}{T_{\text{ref}}}\right)^{\frac{3}{2}} \frac{T_{\text{ref}} + 110.3}{T + 110.3} \quad (7)$$

IV.NUMERICAL SIMULATION

A. There are some assumptions considered to simulate the current model, which are:

B. A density-based solver is carried out because the airflow is very compressible in models such as convergent-divergent nozzles, and the Mach number is important.

C. In terms of time, the model is steady, and the time duration is not considered to solve the problem.

D. It does not consider the effects of gravity on the fluid.

Based on the fact that we use a De Laval nozzle to enter the airflow in the present model, the fluid velocity increases dramatically so that the fluid velocity approaches the sound velocity within the fluid. In such cases, we apply the density-based solution solver where the Mach number is large. The fluid studied is air, which must be defined as the ideal gas, which is not constant when flowing through the nozzle because of the supersonic flow density. For low-speed incompressible flows, pressure-based solvers are used, while density-based solvers are used mostly for high-speed compressible flows. Both are now applicable to an extensive range of flows (from incompressible to highly compressible); however, the roots of the density-based formulation offer it an advantage of accuracy (i.e., shock resolution) over the high-speed compressible flow pressure-based solver [10]. There are two most common turbulence models used in CFD simulations, the k-ε model & the k- ω model. For CFD, both versions are currently used. These two models sometimes have sizeable numerical variations. In most cases, the difference is in convergence time and the number of iterations [11]. For thoroughly turbulent flows, the k–ε model is more feasible. The model performs poorly for complex flows involving high-pressure gradient, separation, and strong streamline curvature. A lack of exposure to adverse pressure gradients is the most essential deficiency. This model is nearly sufficient for initial iterations, initial alternative concept screening, and parametric studies[12]. With an automated transition from a wall feature to a low-Reynolds number formulation based on grid spacing, the k-Ɛ model allows for more precise near-wall treatment. Under adverse pressure gradient conditions, this model performs significantly better for complex boundary layer flows. In numerical stability, k-ω has significant advantages.

For extreme adverse pressure gradient flows, this model underestimates the sum of separation [13]. However, based on the experience of Fluent's present case, temperature outcomes are less sensitive to model choice and seem oblivious to velocity. The effects of pressure seem particularly sensitive to both the choice of model and the mesh. Models are quite different, but it should come as no surprise that each model will generate some variations in outcomes.

V. RESULTS AND DISCUSSION

Table I shows the comparison of values of pressure, temperature, and velocity at the throat obtained from these simulations and the analytical results calculated by using (6) and (7). The simulation results obtained from this model showed good agreement with the computed results.

Table I
Comparision Of Simulated Data With Calculated Data

Chamber pressure (kPa)	Pressure at neck (kPa)		% Difference
	Analytical	This model	
15	11.15	15.10	3.54
11	8.30	13.80	3.93
	Temperature at neck (K)		
15	260.87	252.50	3.20
11	260.87	249.23	4.46
	Velocity at neck (m/s)		
15	320.05	330.0	3.01
11	342.05	328.75	4.0

The red region displays the highest-pressure value in Figure 3, and the blue one shows the lowest. The pressure is close to 15kPa at the inlet, and along the axis, it is decreasing. The pressure decline is slow. The pressure is equivalent to 10 kPa at the outlet. The temperature within the chamber usually is high. Still, under the k-ω turbulence model, we study the flow properties and then the flow properties of inviscid flow, so the temperature at the inlet is maintained at 290K, which is reduced to 180K during the expansion of gases Like in the divergent nozzle section, the surrounding zone temperature is also high as shown in Figure 4. The inlet flow velocity is low in Figure 6 as the pressure of the gases is higher. As the pressure decreases, the velocity increases along the nozzle axis and, at the exit of the nozzle, reaches its peak value of close to 580 m/s. Mach number is a critical parameter that can be utilized for nozzle thrust estimation and separates whether a nozzle is subsonic, sonic, or supersonic. Mach Number at the nozzle's neck is close to 1. The highest reached is at the exit, i.e., 1.8, as shown in figure 5.

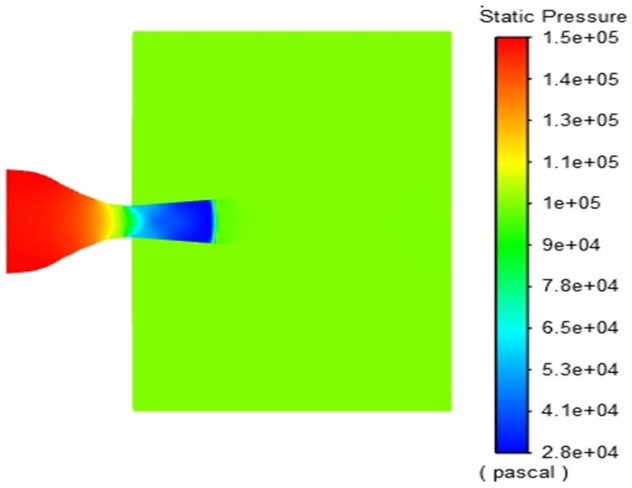

Fig. 3 pressure contour

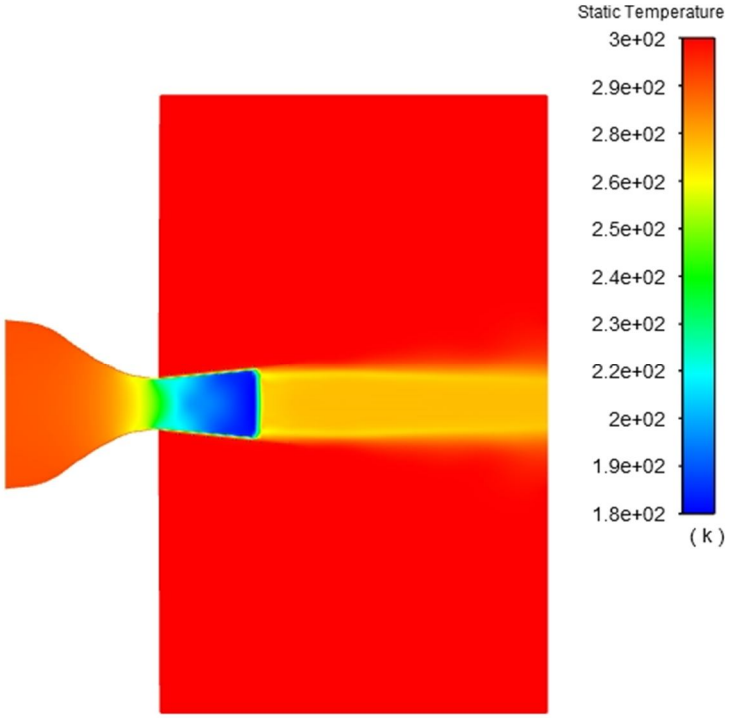

Fig. 4 Temperature contour

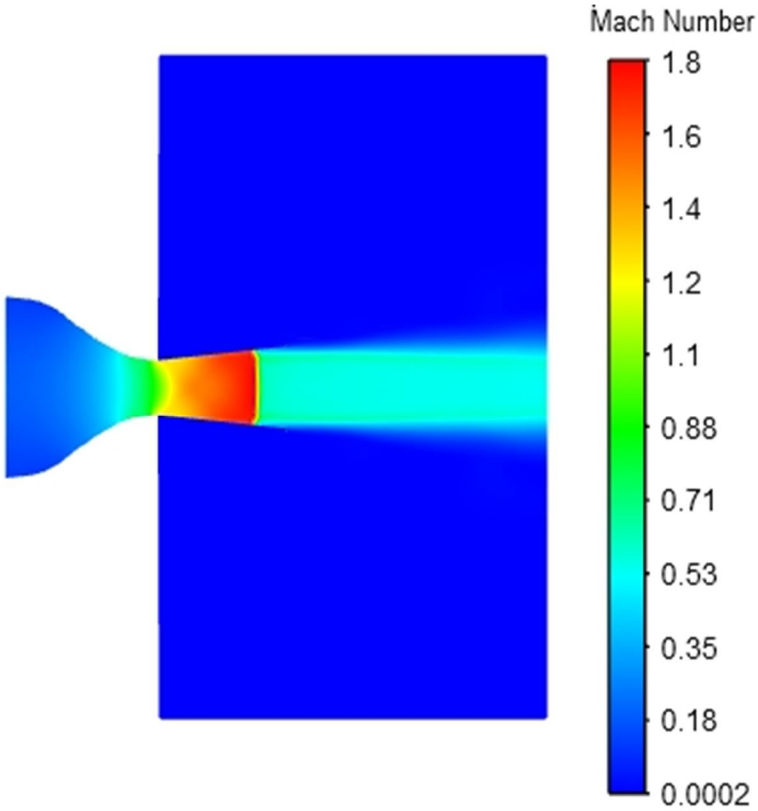

Fig. 5 Mach number contour

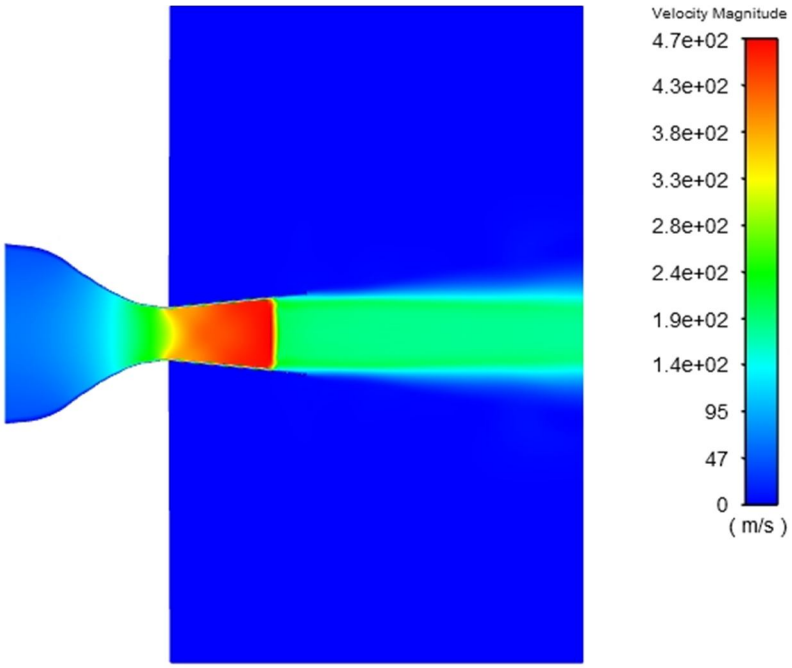

Fig. 6 velocity contour

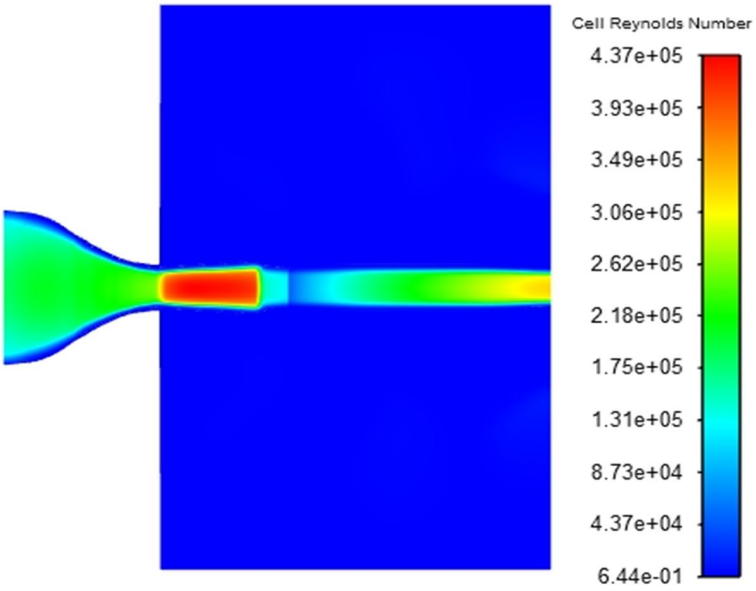

Fig. 7 Reynolds no variation throughout the nozzle

It is evident that Reynolds number is high through the divergent Section, as seen in figure 7. Ultimately, the action of the turbulent kinetic energy normalized by the perfectly extended exit velocity square is addressed. The square of the correctly extended outlet is normalized by velocity. As seen in figure 8, the normalization avoids the apparent effect of rising turbulence as the separate flow velocity increases. Inside the separation shear layers, the normalized turbulent kinetic energy increases and is higher in the shear layer covering the more expansive separation zone. The degree of k is observed to collapse toward the outlet of the nozzle. Fluctuation levels are minimal in the central field of the nozzle. The overall level of the normalized turbulent pressure level increases marginally with the rise of the pressure ratio from 1.25 to 2.5. The direction of the maximum turbulent intensity changes into the nozzle's escape plane.

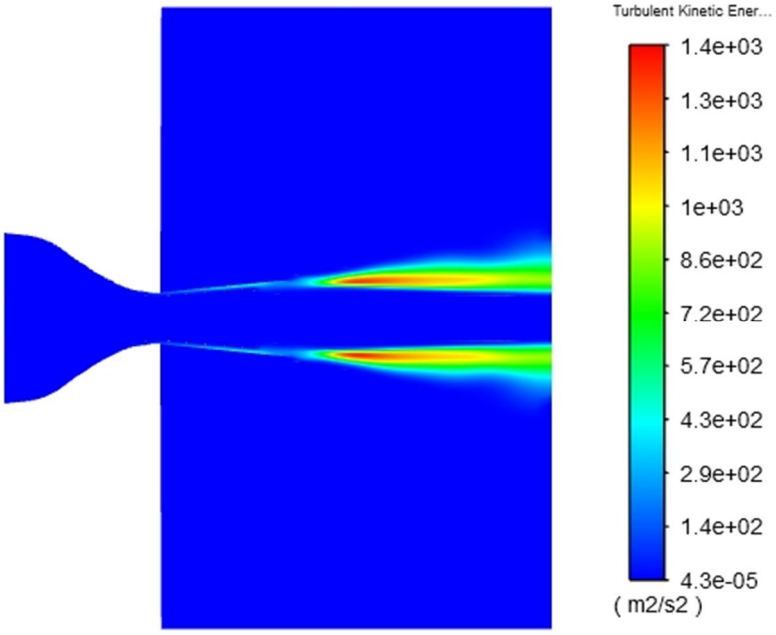

Fig. 8 Turbulent Kinetic Energy contour

VI. CONCLUSION

A detailed study was conducted on the effect of inlet pressure variation on the Mach number and shock produced inside the nozzle using the standard k-ω turbulence model. The pressure measurements were used to validate the shock location and the expansion of the component gases in the divergent nozzle section. In this geometry, the maximum Mach number is the minimum pressure in two turbulence models at the same location. This converging-diverging geometry does not cause more than this number to hit the Mach number. As the speed after the nozzle is supersonic, the Mach number should be more than one after the throat, while in both models, the Mach number is 1 in the throat, but in comparison to the k- ω model, the k-ε model earns higher average values of the Mach number. It has been found that there must be equal pressure in the throat and backpressure (or very close). Green areas have the same Mach number value aftershock and throat. As predicted, the results of numerical simulation for measured data are not fully matched. The nozzle's surrounding atmosphere is often carried out during the formation of the shock wave. Within the nozzle but near to the exit, a shock was detected. It is clear that wall frictions are not present as the shock form is smooth. Therefore, simulations using the standard k-ε turbulence model provide more practical values than simulations conducted under conditions of inviscid flow.

REFERENCES

[1] Hunter, C. A., "Experimental, Theoretical, and Computational Investigation of Separated Nozzle Flows," AIAA Paper 98- 3107,1998.
[2] Carlson, J. R., "A Nozzle Internal Performance Prediction Method," NASA TP 3221, 1992.
[3] Xiao, Q., Tsai, H. M., and Liu, F., "Computation of Transonic Diffuser Flows by a Lagged k-! Turbulence Model," Journal of Propulsion and Power, Vol. 19, No. 3, 2003, pp. 473–483.
[4] Romine, G. L., "Nozzle Flow Separation," AIAA Journal, Vol. 36, No. 9, 1998, pp. 1618–1625.
[5] Papamoschou, D., "Mixing Enhancement Using Axial Flow," AIAA Paper 2000-0093, Jan. 2000.
[6] Papamoschou, D., and Zill, A., "Fundamental Investigation of Supersonic Nozzle Flow Separation," AIAA Paper 2004-1111, Jan. 2004.
[7] Bourgoing, A., and Reijasse, P., "Experimental Analysis of Unsteady Flows in a Supersonic Planar Nozzle," International Symposium on Shock Waves, Vol. 14, No. 4, Springer, New York, 2001, pp. 251–258.
[8] Reijasse, P., and Bourgoing, A., "Unsteady and Asymmetry of ShockInduced Separation in a Two-Dimensional Planar Nozzle," AIAA Paper 99-3694, 1999.
[9] Deck, S., Hollard, R., and Guillen, Ph., "Numerical Simulation of Steady and Unsteady Separated Nozzle Flows," AIAA 2002-0406,2002.
[10] Á. Veress, and J. Rohács. (, 2011). Application of Finite Volume Method in Fluid Dynamics and Inverse Design based Optimization. Budapest University of Technology and Economics. [Online]. Available: www.intechopen.com/download/pdf/33899.
[11] F. Menter and Y. Egorov, "The scale-adaptive simulation method for unsteady turbulent flow predictions. Part 1: Theory and model description," Flow, Turbulence and Combustion, vol. 85, pp. 113-138.
[12] G. Mylavarapu et al., "Validation of computational fluid dynamics methodology used for human upper airway flow simulations," Journal of Biomechanics, vol. 42, pp. 1553-1559, 2009.
[13] F. R. Menter, "Performance of popular turbulence models for attached and separated adverse pressure-gradient flows," Aiaa Journal, vol. 30, pp. 2066-2072, Aug. 1992.

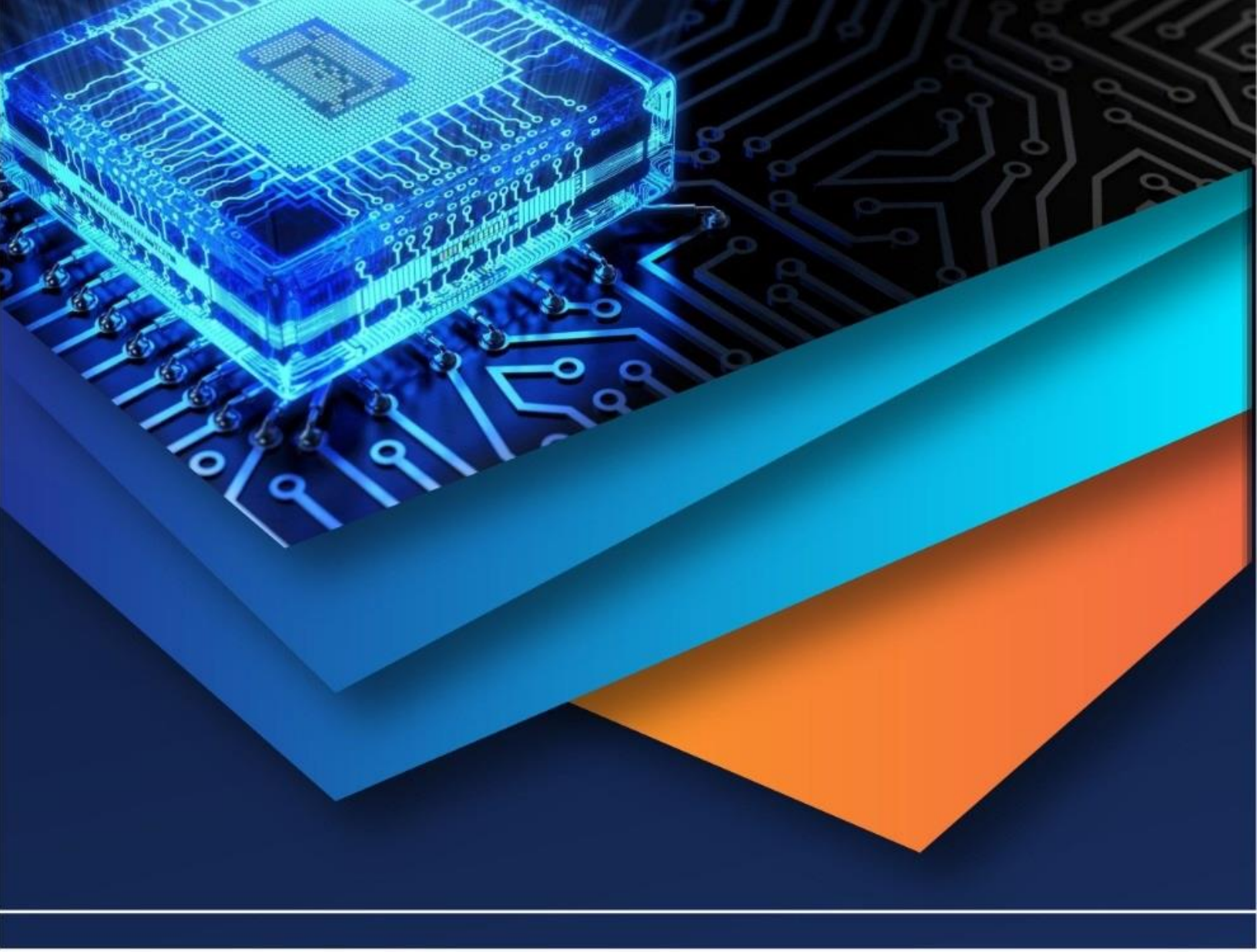

10.22214/IJRASET

45.98

IMPACT FACTOR: 7.129

IMPACT FACTOR: 7.429

INTERNATIONAL JOURNAL FOR RESEARCH

IN APPLIED SCIENCE & ENGINEERING TECHNOLOGY